Neuroscience

http://www.aimspress.com/journal/neuroscience

AIMS Neuroscience, 3 (2): 163–180.
DOI: 10.3934/Neuroscience.2016.2.163
Received: 25 January 2016,
Accepted: 28 April 2016,
Published: 4 May 2016

Research Article

Modeling the Antipodal Connectivity Structure of Neural Communities

Bayazit Karaman[1] **R. Murat Demirer**[2] **Coskun Bayrak**[3,*] **and M. Mert Su**[4]

[1] Computer Science Department, University of Arkansas at Little Rock, 2801 S University Ave, Little Rock, AR, USA

[2] Industrial and System Engineering, Uskudar University, Istanbul, TURKEY

[3] Computer Science Department, University of Arkansas at Little Rock, 2801 S University Ave, Little Rock, AR, USA

[4] University of Arkansas at Little Rock, 2801 S University Ave, Little Rock, AR, USA

[*] **Correspondence:** cxbayrak@ualr.edu; Tel: +1-501-569-8137; Fax: +1-501-569-8144.

Abstract:
Recent studies support the theory of the brain being composed of modules and certain nodes establishing connections between the modules [1, 2, 3]. The existence of such connections can only be identified by conducting a detailed investigation with sophisticated tools. Therefore, in this manuscript we provide a new mathematical model to indicate the functional dependency, which supports the idea of information exchange between the neural modules at the highest spatial and hierarchical level of bottom-up processes using EEG (ElectroEncephaloGraphy) [4]. The developed model is to study the functional dependencies between different regions of the cortex is based on the Borsuk-Ulam's antipodal symmetry theorem. It is a mathematical model complemented with an innovative algorithm, called Projection based on Normalized Transformation (PNT), to show the existence of unique neural activity pattern known as the Antipodal Connectivity. For validating of the model, EEG data collected from a total of 50 experiments with the participation of 18 different test subjects was used to measure the effectiveness and accuracy of method. Using the data collected from the subjects in different stages (active or resting) of the brain, the Antipodal Hub Neurons (AHNs) were captured and compared to determine the ratio of fluctuation under different conditions and whether or not the stimulus has any role in antipodal neural connectivity. Although the preliminary results are not conclusive, we have successfully identified the existence of antipodal behavioral patterns in neural activities.

Keywords: EEG, Antipodal Symmetry, Borsuk-Ulam Theorem, Antipodal Connectivity, PNT, AHNs, Neural Communities, Antipodal Hub Neurons

1. Introduction

A neural network, which has the property of a modular/colonial structure and controls the information behavior of a human, is governed with a set of organizational principles. The structure in this modular/colonial environment is hierarchical and connections are established through the mutually exclusive nodes. We hypothesize that the decision mechanism behind a cognitive process takes place at the highest hierarchical and spatial level. The hierarchy is present between both functional and structural connections such that the neural signal paths emerges in white matter and concludes at gray matter. Such understanding is analogous to the wiring principles of the cerebrum that white matter accommodates the myelinated axons, which carry impulses to the cerebral cortex. (This generalization is also supported by the widely-accepted convention that the white matter accommodates the myelinated axons, which carry impulses to the cerebral cortex.) In this context, we are trying to unify the cognitive decision-making mechanism rather than trying to distinguish it between certain regions of the brain. The complexity of the cognitive decision mechanism can be observed in patients after a brain surgery. Although removing some portions of the brain may stop the progression of diseases, the brain loses some of its previous capabilities that were not related to that region, after the surgery. This suggests that there is a higher-level hierarchy in decision-making. Note: The decision-making mentioned here should not be confused with the decisions related to conscious choices. We assume that storing or sending information between neural populations is an internal cognitive decision-making process that starts at the lowest hierarchical structural level and concludes at the highest level in the hierarchy before any related task is completed. The rationale behind this approach lies at the very foundation of how the brain operates. Brain is constantly active whether it is in resting or active state because of the continuous blood-flow even in the deep sleep stage known as N3, which can be observed with EEG. Therefore, the brain may operate in a much more complicated and unified fashion rather than depending on single regional interactions for cognitive decision-making. Existing methods in neuroscience have made important advances in the last two decades with the introduction of functional Magnetic Resonance Imaging (fMRI), diffusion-MRI, and arterial spin labeling. Inductive reasoning constitutes the foundational background for these technologies that the final conclusion depends on examining the relationship between smaller fragments of a larger implication. The complexity of the relationship between structural and functional connectivity amongst the neural communities makes inductive reasoning extremely challenging in providing a solid understanding of the cognitive functionality. Although the methods have been proven to be effective in neural analysis, one fundamental disadvantage is in the defining of the size of the fragments. This is a tedious task because of the immense number (100 billion) of neurons in the mammalian brain. Moreover, the brain operates non-linearly, inferring that the size of the communities is dynamic and the contributions of these communities do not have identical effects on the final conclusion. We believe the size, boundary, hierarchy and assignments/responsibilities of neural communities are dynamic, in opposition to the general concept of predetermined size of modules. Therefore, in spite of the general convention of identifying the closely coupled neurons as neural modules, we prefer a new term; neural communities because the word community not only symbolizes the dynamic relationships and associations but also emphasizes the hierarchical foundation of it. Therefore, a new approach based on deductive reasoning is developed for neural analysis. Such an approach will represent the activity of the neural populations more realistically because of the following reasons:

1. Hemispherical shape of the brain and tendency of the electric current to flow on the surface of a curved conductor
2. Proven modular connectivity between neural populations
3. Overall decision-making mechanism is at the highest spatial level due to Reason 1.

A schematic diagram showing the differences between inductive and deductive reasoning is provided in Fig.1.

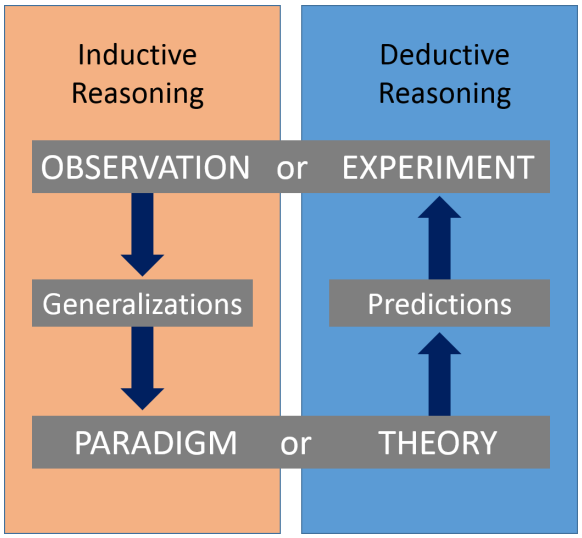

Figure 1. The flow diagrams of inductive and deductive reasoning

For the reasons explained above, EEG emerges as an excellent candidate for utilizing the deductive approach because of the data collection method. However, the existing EEG data analysis methods are not reliable for this task and an enhanced and innovative data analysis models associated with a proper tool is needed in order to:

1. Contemplate the voltage emerging from neural electrical activity via the limited cross-sectional area of the electrode in a single dimension, and
2. Collect EEG data from separate electrodes (also called channels or sensors) for simultaneous correlation in the third-dimensional complex domain.

2. Theoretical Foundation

Understanding physiological process in the brain requires formal system models. Therefore, the connectivity is a core component of such models. According to a recent study [5], 70% of all information within the cortical regions in the brain passed through only 20% of these regions neurons. In other words, the 20% of this ration are referred to as Hub-neurons. Recent studies conducted at Indiana University [5] Hub-neurons not only aid in understanding the information processing behavior of the cortex but also reveals some feedback on the impact of neurogenerative diseases that effects the network. Hub-neurons are known to be information rich and have a direct or indirect link in the process of

forming the antipodal connections. Although the existence of Hub-neurons, which carry the majority of information between cortical regions in the brain, have been reported in [6, 7, 8, 9], the first known mathematical model showing their existence was introduced by [8, 9]. This study, therefore, proposes the introduction of a potential cognitive biomarker called Antipodal Hub Neurons (AHNs) along with the associated hypothesis called antipodal connectivity of neural communities, in an effort to provide a better perspective in cognitive dynamics (Fig.2).

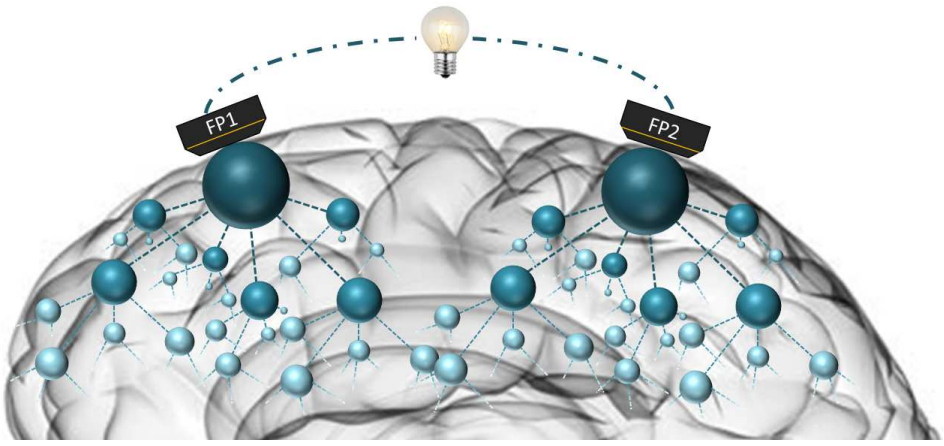

Figure 2. A visual representation of the colonial and collective information bridging antipodal connectivity detected between the EEG electrodes, FP1 and FP2. Information is conveyed between the neural communities until reaching the final stage point/area underneath the electrodes.

The complexity of the brain is complemented with the activities resulting from neural communication and coordination. Extracting details of the process is inadequate if a simple analysis is conducted. Therefore, a comprehensive analysis with a solid theoretical foundation should be conducted at different levels to capture the details. Hence, a theoretical model, based on the potentials of Gauss' Law and Borsuk-Ulam theorem, were adapted to project single dimensional EEG data to third-dimension by complex analysis thus, the detailed communication and coordination of neural communities at the highest spatial and hierarchical level can be examined.

2.1. Gauss' Law

Gauss Law states that "the total electric flux (ϕ) out of a closed surface is equal to the charge (Q) enclosed divided by the electrical permittivity (ϵ)", i.e. ϕ=Q/ϵ [10, 11] (Fig. 3). The electrical charges inside a solid closed surface (for example; skull) will move freely until the excess charges gather on the surface of the conductor. The charged particles will continue their motion until the electric field inside the conductor will be zero, which is known as electrostatic equilibrium.

Generally speaking, Gauss Law [12] states that the positive electrical charge density inside a conductor sphere creates an electrical field pointing outward. A similar assumption can be made for the brain, which resembles a hemisphere, since a certain amount of electrical current is flowing through the surface in a given time due to the continuous activity of the neural communities. However, the electrostatic equilibrium can only be held for a very short period of time as a result of this perpetual activity. The cerebral cortex and the cerebrospinal fluid are electrically conductive [13]. Therefore,

Gauss Law is an excellent representation of how the electrical charges gather on the outer surface of the conductive margin of the brain, creating an electric field (Fig. 3).

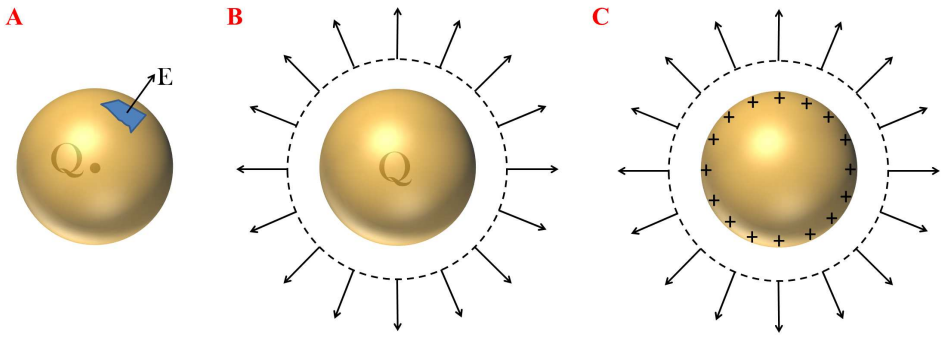

Figure 3. A – Visual representation of Gauss Flux Theorem showing the electrical field (E) generated by a positive point charge (Q) pointing outward, which is perpendicular to the area in blue. B – Uniform positive charge density (Q) of a conducting sphere creating an electrical field surrounding the charge density. C – The positive electrical charges inside the closed surface gathering on the surface of the solid electrical conductor. These charges create an outward electrical field surrounding the sphere.

2.2. Borsuk-Ulam Theorem

The antipodal connectivity hypothesis is based on the antipodal-points concept of the Borsuk-Ulam theorem[14]. The theorem describes the existence of a pair of points, which are 180 degree apart on a spherical surface, having the identical shared value at a given time. Accordingly, we hypothesize that this principle is also true between the neural communities. Hence, there exists a pair of neural communities connected through a set of hub-neurons that are apart at the highest spatial level and share identical information simultaneously. This is credible evidence indicating that a paired connection based on shared value exists between those communities. These pairs are defined as the AHNs and the associated sets of communications are defined as antipodal connectivity of neural communities. A schematic representation of this hypothesis is provided in Fig. 4.

Borsuk-Ulam Theorem is the one most commonly used in complex analysis and algebraic topology to extract details [15, 16]. The formal definition of the theorem, which was introduced in 1933, states, "Every continuous mapping of n-dimensional sphere, S^n into n-dimensional Euclidean space, R^n, identifies a pair of antipodes". More specifically, for every continuous mapping $f : S^n \to R^n$ there exists a point $x \in S^n$ such that $f(x) = f(-x)$.

The behavior of the neural populations is intricate to understand with raw EEG data. Therefore, discovering the antipodal points to understand the dynamically cohesive nature of coupled neurons needs a preprocessing step, which is crucial for neural interactivity analysis and mapping [17, 18]. For this step, the data needs to be projected into a higher dimension through the use of the Borsuk-Ulam theorem.

The identification of antipodal structures is a significant part of the dynamically cohesive nature of coupled neurons. For instance, if there is a change in the number of antipodal pairs for different activity stages of the brain, it suggests that there exists a pattern of cohesive cooperation between the

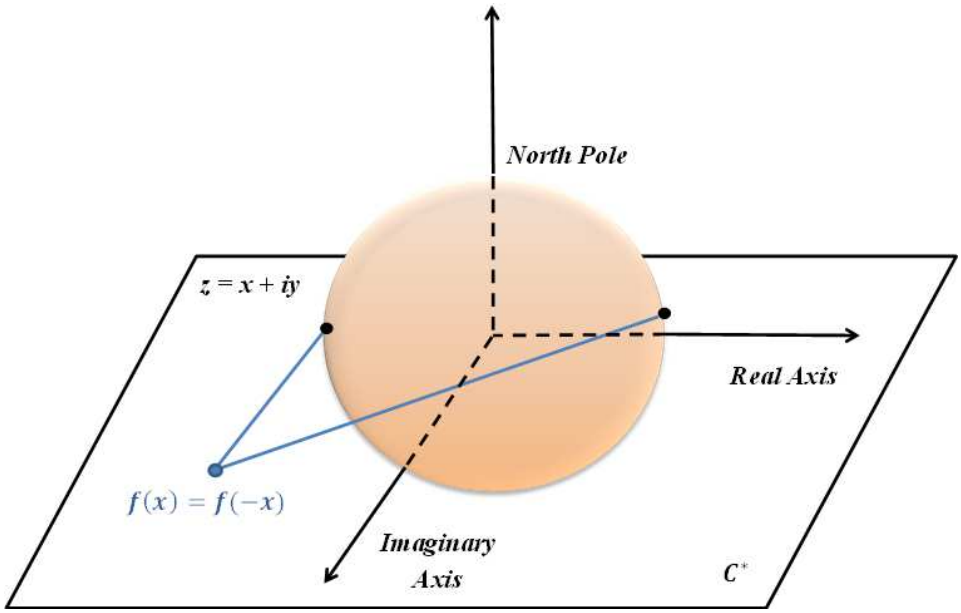

Figure 4. Visual representation of Borsuk-Ulam theorem. Two antipodal points (black dots) on the complex sphere projected to a single point on the complex punctured plane.

communities. This is calculated by evaluating the existence of antipodal points between the different EEG channels at a given time (t). Furthermore, the existence of antipodal points is evaluated in the proceeding discreet-time-step ($t + 1$) until all the selected window is processed ($t \in \{1, 2, 3, ..., W\}$) where W is the window length. The analytic signals from multichannel EEG data are compared at every time-step ($t = 1, 2, 3, ..., W$) by using a mathematical model called PNT, which is based on Borsuk-Ulam theorem. The selection of W is based on the given stimulus (i.e. "resting" and "active").

3. Mathematical foundation of PNT Model

Expanding on the Borsuk-Ulam theorem, the PNT model provides a mathematical formulation for analyzing the antipodal connectivity at the highest hierarchical level. PNT is designed to extract the structural patterns in the cognitive decision mechanism using EEG test data recorded with different stimuli. PNT is a three-step processing algorithm. Order of the steps is as follows; 1- Transformation, 2- Normalization, and 3- Projection. The phase information is obtained by using transformation, which is required for assessment of the synchronization between sensors. Additionally, Hilbert transformation yields to an analytic signal (R^2), which has only positive frequencies. The analytic signal is free of negative frequency content which is physically meaningless. Normalization is used to confine the transformed data into a unit disk which enables uniform processing for all data sets. Finally, the normalized EEG signal is mapped on the unit sphere with the help of Projection. The resulting mathematical formulation for PNT process is given below.

In Eq. 1, EEG data, which includes the amplitudes, is converted into analytical signal using Hilbert transformation ($\mathcal{H}$) to extract complex attributes channel by channel, $f \in R \rightarrow f \in \mathbb{C}(D)$, i.e. [19].

$$f(x, t) \xrightarrow{\mathcal{H}} f(x + iy, t) \tag{1}$$

where, x is the original signal and y is Hilbert transform of the original data which are real and imaginary components of the analytic signal on the complex plain respectively.

Driving from the formal definition, the function G, a closed unit disk on the upper hemisphere, can be defined by the function f in the complex domain as [15]:

$$f(x+iy,t) = G(x, y, \sqrt{1-x^2-y^2}, t) \tag{2}$$

where, $\sqrt{1-x^2-y^2}$ is the z component in the Cartesian coordinate system. This statement is reversible if the function f is one-to-one and onto, such that a function f that exists on a complex domain (R^n), can be projected onto a sphere by the function G [15]. The high level representation of PNT method is shown in Fig. 5.

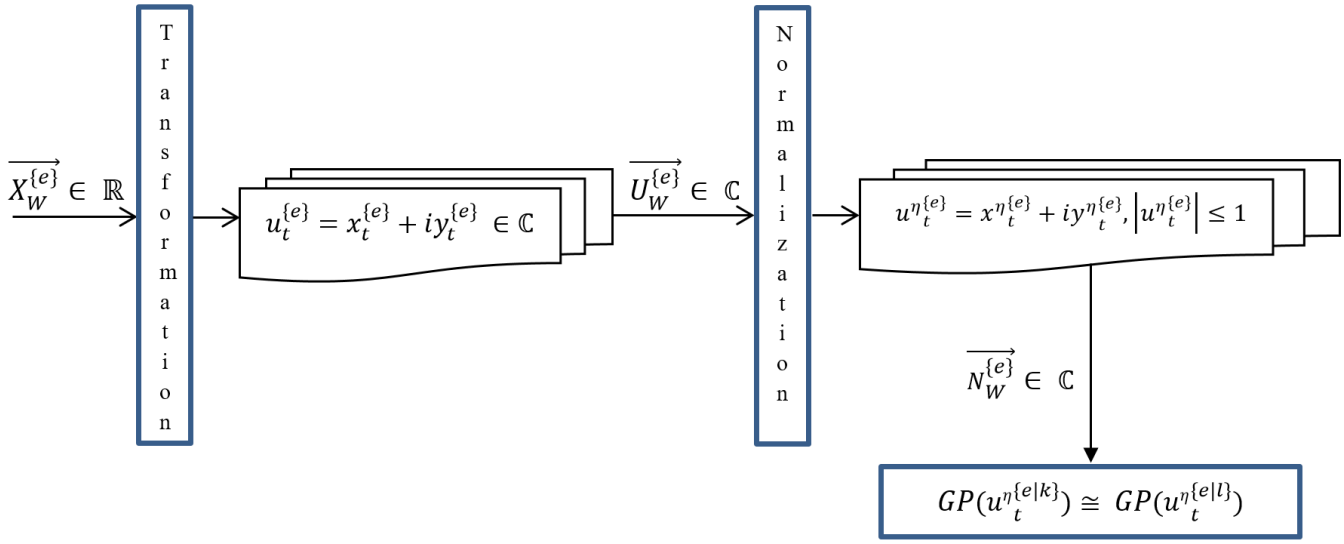

Figure 5. The high-level schematic representation of PNT method.

The general formula of the PNT method is given in Eq. (3).

$$GP_t^{\{e\}}\left\{\overrightarrow{N_W^{\{e\}}}\left\{\overrightarrow{U_W^{\{e\}}}\{\overrightarrow{X_W^{\{e\}}}\}\right\}\right\} \tag{3}$$

where $U : \mathbb{R} \to \mathbb{C}$, $\mathbf{W}$ is the window size, and t is the discrete time-step, which is between 1 and $\mathbf{W}$. i.e., $1 \leq t \leq W \in t = \{1, 2, 3, ..., W\}$. e denotes the electrode number out of total number of electrodes. i.e., $e = \{k, l \mid Fp1, Fp2, Cz, ..., Oz, O2\}$.

The data collected with 14-channel EEG system to test the capabilities of PNT method is processed in a segmented fashion, where each data (signal) segment is composed of data points (p) (in our case we used 1024 data points, due to the stimulus used in the experimentation). Thus, X is a matrix with rows (r) (in our case we used 14 rows) and p columns, as shown in Eq. (4).

$$\overrightarrow{X_W^{\{e\}}} = \{x_1^{\{e\}}, x_2^{\{e\}}, ..., x_W^{\{e\}}\} \tag{4}$$

where $\overrightarrow{\boldsymbol{X}_{\boldsymbol{W}}^{\{e\}}}$, raw EEG data, is transformed vector by vector using Hilbert Transform. Therefore, the output signal, $\mathbf{U}$, is also a matrix, which has the same dimension as in Eq. (5).

$$\overrightarrow{U_W^{\{e\}}} = \{x_1^{\{e\}} + y_1^{\{e\}}, x_2^{\{e\}} + y_2^{\{e\}}, ..., x_W^{\{e\}} + y_W^{\{e\}}\} \tag{5}$$

where $x_t^{\{e\}} + y_t^{\{e\}}$ was defined as $u_t^{\{e\}}$, therefore the general formula of Transformed data as given in Eq. (6).

$$\overrightarrow{U_W^{\{e\}}} = \{u_1^{\{e\}}, u_2^{\{e\}}, ..., u_W^{\{e\}}\} \tag{6}$$

According to Eq. (2), one fundamental constraints of projection onto the upper hemisphere is that the real and imaginary data must be smaller than 1. Therefore, the normalization is performed to prepare the data for projection. In other words, performing normalization for each vector produces an output signal, which is a unit circle in complex plane, as shown in Eq. (7).

$$\overrightarrow{N_W^{\{e\}}} = \{u_1^{\eta^{\{e\}}}, u_2^{\eta^{\{e\}}}, ..., u_W^{\eta^{\{e\}}}\} \tag{7}$$

Calculating the third dimension using the real and imaginary parts of data is to monitor the closely coupled neural activities. Therefore, function $G : R^2 \rightarrow S^2$ is defined. The main objective is to discover two electrode pairs having equal PNT values in three-dimensions at time, t. Hence,

$$G_t(x_t^{\eta^{\{e\}}}, y_t^{\eta^{\{e\}}}, \sqrt{1 - x_t^{\eta^2} - y_t^{\eta^2}}) \tag{8}$$

where;
$x_t^{\{e\}}$: The real part of the data collected from sensor **e** at time **t**.
$x_t^{\eta^{\{e\}}}$: The real part of the data collected from sensor **e** at time **t** after normalization.
$y_t^{\{e\}}$: The imaginary part of the data from sensor **e** at time **t**.
$y_t^{\eta^{\{e\}}}$: The imaginary part of the data from sensor **e** at time **t** after normalization.

The GP_t function is the simplified version of Eq. (8). The function requires two input values, which are real and imaginary parts of the specific data to calculate the third dimension value, as shown in Eq. (9).

$$GP_t = \sqrt{1 - x_t^{\eta^2} - y_t^{\eta^2}} \tag{9}$$

Once the complex attributes of EEG data is extracted using Hilbert transform, they are projected onto the upper hemisphere using Eq. (9). This process is repeated for every channel at each time-step. Thus, the 3-D values are calculated in spatial-temporal domain from 1-D EEG amplitudes. When the degree of similarity between 3D values for channel-pairs are closely identical (≤ 0.00001) at a time-step, ***t***, two remote communities at the highest spatial level (right below the electrodes) are assumed to have bridged a connection at the highest hierarchical level. Such neural communities are defined as AHNs. Hence, the following formal definition holds.

Definition-1: *For all electrodes, there exist two different sensors (k and l), which have approximately the same 3-D values at time* ***t*** (Eq. (10)).

$$\forall\ e\ \exists\ k, l \ni GP_t(u_t^{\eta^{\{e|k\}}}) \cong GP_t(u_t^{\eta^{\{e|l\}}}) \tag{10}$$

With respect to the formal foundation established for PNT model, it is safe to make the following observation.

Observation-1: *In the spatial-temporal complex domain, there exists a pair of sensors whose projected 3-D values are equal with 5-digit precision in terms of real and imaginary parts.*

4. Method

Since the approach and the mathematical model provided in this study have not been tested before, evaluation of the measurable outcomes is purely based on this experiment. We initially hypothesized that the amount of Antipodal Hub Neurons (AHN) varies according to the brain's current stage, which is active or resting. In order to test this hypothesis, we conducted this comprehensive experiment on normal subjects with different age groups and sexes. In our study we also hypothesized that the number and meaning of the AHNs can change with the frequency bands of the EEG data. The best known and used frequency bands of the EEG data is between 1-60 Hz, dividing the EEG data into five main bands, i.e., delta (1-4 Hz), theta (4-8 Hz), alpha (8-13 Hz), beta (13-30 Hz) and gamma (30-60 Hz) [20]. The waves, delta through beta, are associated with problem solving, memory functions, relaxation, and creativity [21].

4.1. Materials and Environment

For the experimental setup, a EEG system with 14 channels is used to record the data. It has the same properties of an international 10-20 system with a channel configuration as follows; AF3, F7, F3, FC5, T7, P7, O1, O2, P8, T8, FC6, F4, F8, and AF4. The EEGLAB which is an open-source and the most widely used toolbox in the world to analyze the EEG data [22] was used to filter the data .

The data collection environment is designed in such a way to avoid any noise and artifacts. Therefore, without causing any distraction a list containing 26 letters were laid out randomly on a cardboard display that was placed in front of the test subjects at a distance of approximately five feet (see Fig. 6).

4.2. Participants

After obtaining the IRB certification, 18 individuals of different age groups and sexes (11 males and 7 females) were recruited to participate in the data recording. Subjects were given small condiments 45 minutes prior to the experiment. Thus, the subjects are assumed to accomplish the tasks under similar physiological states. The age range for the male and female participants are 25-56 (average 28.1) and 21-45 (average 27.9), respectively.

4.3. Procedure

As shown in Fig. 6, subjects were asked to follow a certain procedure to complete experiments. The steps were explained to the subjects before the experimentation in order to unify the testing procedure.

1. Subjects start the procedure with their eyes closed while listening to background music.
2. Data recording starts after a short while ensuring that the subjects were only concentrating on the music.
3. After 10 seconds, a trigger signal goes off notifying the subjects to open their eyes and start searching for the letters of a predetermined 5-letter meaningful word in order in the least possible

time. Up to this point, subjects had not seen the letters on the cardboard hence; the process would require a certain level of challenge.

4. Upon finding the word on the cardboard subjects snap their fingers as a confirmation of accomplishing the task.

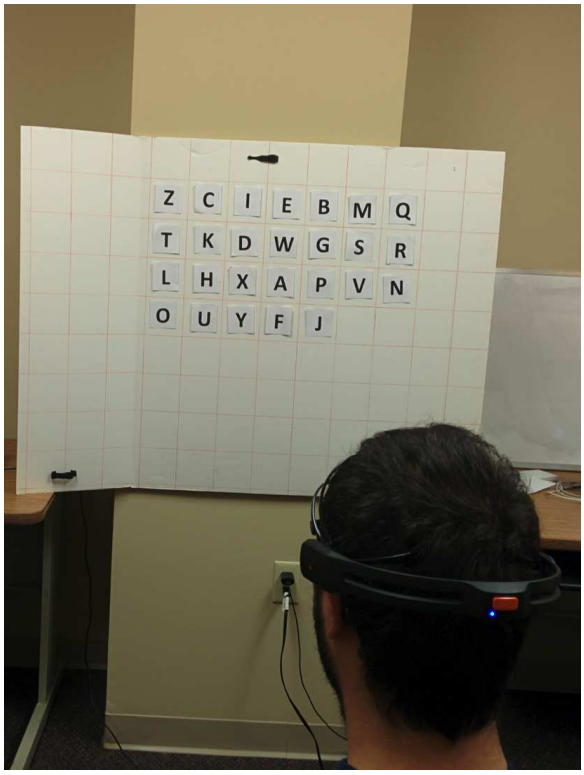

Figure 6. EEG data collection with arbitrarily laid out letters after a resting period. Test subject (right) was trying to find letters on the cardboard while data was analyzed by the technician (left).

Calm classical music is used as background noise to help subjects relax and to foster an idle state of the brain as much as possible [23, 24]. The initial 10-second period was determined as the control data where brain activity was assumed to be minimum/default. In this context, a quiet environment was not desired since the subjects might indulge in other thought processes. Three unique 5-letter words were chosen for the test, which consisted dissimilar letters for each word.

4.4. Analysis

In total, 54 experiments were conducted. The participants were asked to find letters in the correct order under 1 minute. Although, there was no limitation for the duration of experiments, finding each of the 5-letter words lasted 8 seconds on average. During Experiment-3, participants 1, 3, 5, and 18 completed the task in an amount of time relatively shorter than required ($\geq 8secs$) therefore extracting meaningful information from that data set was not possible. Hence, they were excluded from the results due to the unreliable information they might carry. The collected data were analyzed using a FIR filter implemented in EEGLab [25] for noise reduction and band selection for the related brain activity.

5. Results and Discussion

Using PNT method, a total of 50 experiments were analyzed to show the existence of AHN network structure in the brain network. The significant increase in the number of AHNs in active stage for Experiment-2 with Subject-5, and Experiments 2 and 3 with Subject-6 were detected, these findings were defined as outliers and excluded from the result. Fig. 7 shows the histogram of PNT results for 47 experiments where significant increase in the number of AHNs were detected in active brain stage relative to the resting stage. The majority of AHNs are encountered in frontal and parietal cortex. The total number of AHNs for all the test subjects during the resting stage and active stage are 1564 and 2957, respectively. In other words, the average number of AHNs per experiment during the resting stage and active stage are 33.277 and 62.915, respectively. These results confirm that the AHNs increased approximately 2 times on average during the active stage. Additionally, the standard deviation of AHN counts for each experiment during the resting stage is 23.01, while it is 40.786 at active stage.

Considering the results presented in Fig. 8 and in Table 1, we encounter a similar conclusion in that all of the test subjects (mean) showed an increase in activity and number of AHNs while their brain was engaged with some tasks. Additionally, a randomly generated (Gaussian distribution) data set was processed with PNT method. For consistency, each data set was produced to contain an equal number of data points as the real EEG waveforms collected during the experiments. The AHN counts for the data set were significantly less than that of the EEG data collected from the subjects which verified that the occurrence of antipodal connectivity is not random but depends on the level of activity. This confirms the reliability of the proposed formal methodology. provided in this study.

Due to the non-consistency pattern, i.e.,there were no consistent number of AHNs detected for the test groups (see Table 1) used in the experimentation, a statistical analysis was conducted to compare the significance of average numbers of AHNs encountered during the resting stage with active stage and resting stage with randomly generated data per subject. Since differences between data sets(randomly generated, active, and resting stages) individually were not normally distributed, the non-parametric statistical method (Mann-Whitney U test) was used. Firstly, the Mann-Whitney U test was applied to the resting and active stages data sets to reject the null hypothesis, since it states that two data sets are not significantly different at $p \leq 0.01$(probability).The default critical value of U is 81 when $p \leq 0.01$ and $n=19$. With respect to the comparative analysis performed on different data (resting-active) sets,the U-value calculated to be 54.5 which is smaller than the critical value of U at $p \leq 0.01$, hence the null hypothesis was rejected. Similarly, the random generated and resting stage data sets revealed U-value of 6 which is smaller than the critical value of U at $p \leq 0.01$. Nonetheless, the final outcome of the analysis indicated a significance differences between randomly generated data and resting stage data and the resting stage data with active stage.

It is worth noting that, an EEG system with more channels may be more efficient to capture more AHNs during the active stage, since the brain is operating in a non-linear fashion as mentioned the non-stationarity of the EEG signals can be observed during the change in alertness and wakefulness [26]. In other words, electrical activity of the brain varies with the level of processing.

Out of hundreds of AHN pairs detected by the PNT algorithm, an AHN pair captured by the Sensors, F4 and O2 is illustrated in Fig. 9. PNT detected this AHN pair at t = 1.66 seconds. Therefore, in order to test the validity of the PNT method, the amplitudes of the concurrent EEG values are compared to detect any similarities for the same sensors as a control measure.

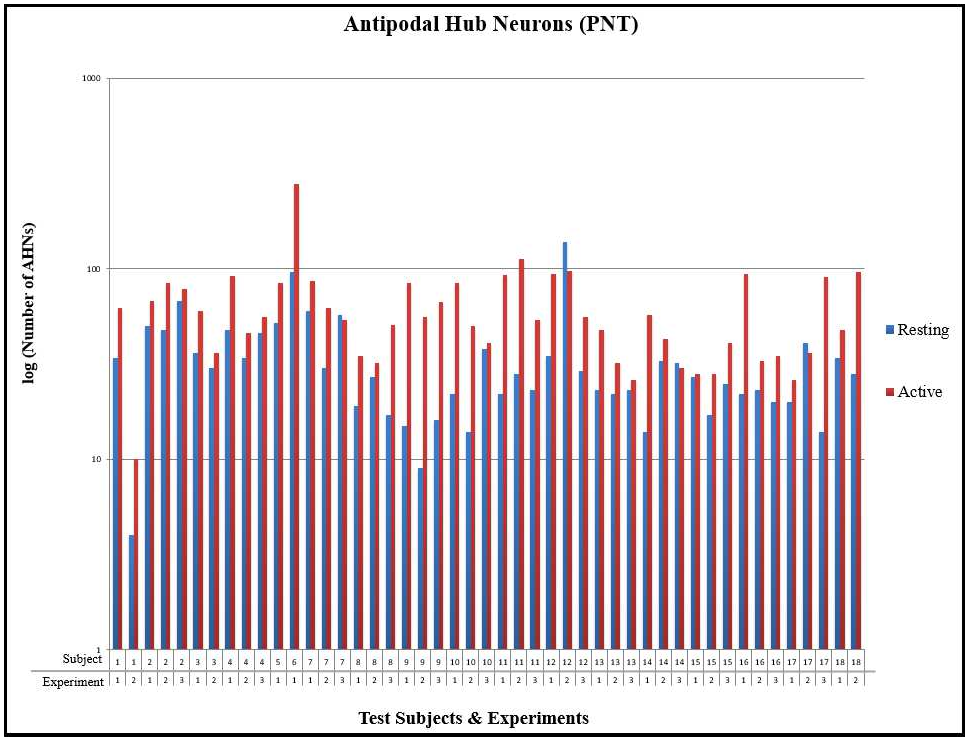

Figure 7. Antipodal connectivity results in 1-31 Hz band for 47 experiments. Results indicate that approximately 92% of the experiments show increased activity and number of AHNs while the brain was engaged with the task.

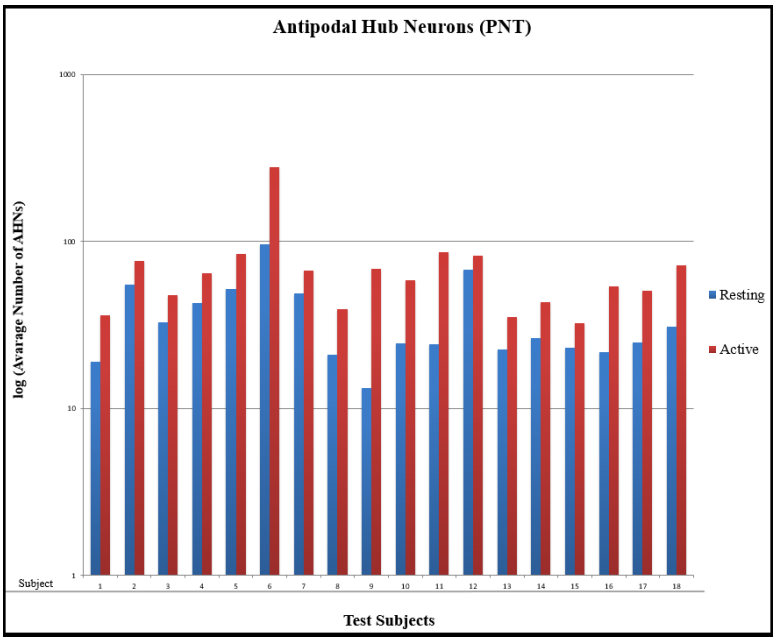

Figure 8. The average number of AHNs in 1-31 Hz band for 18 subjects individually.

Table 1. The average number of AHNs (random, resting, and active) per subject

	Number of Antipodal Hub Neurons		
Subject Number	Randomly Generated	Resting Stage	Active Stage
1	8	19	36
2	17	55	77
3	14	33	48
4	11	43	65
5	18	52	84
6	3	96	280
7	6	49	67
8	2	21	36
9	7	13	69
10	3	25	58
11	19	24	86
12	11	68	83
13	19	23	35
14	6	26	43
15	8	23	32
16	3	22	54
17	9	25	51
18	4	31	72

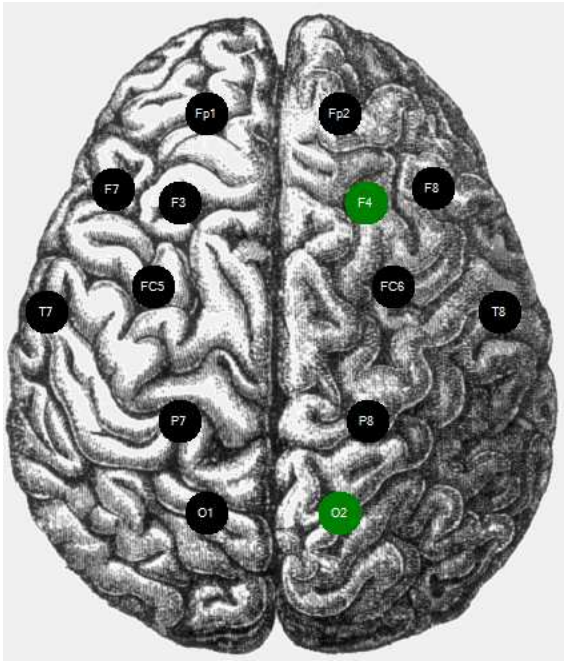

Figure 9. The AHN pair detected by Sensors F4 and 02 at t=1.66 seconds.

The compared data sets show that the concurrent raw EEG amplitudes are dissimilar while the PNT values are identical with a precision of ten thousandths. Table 2 shows the comparison between the values of three AHNs detected with PNT (t=1.66, 12.65, 14.48 seconds) and the amplitudes of the raw EEG data for the same sensor pair (F4 and O2). These results confirm that raw EEG data is not sufficient to discover AHNs without using the PNT. Additionally, the increase in AHN counts in the active stage compared to that of the resting stage strongly suggests that there is a pattern. Although, such a pattern is not fully understood yet, the increase in the correlated pairs detected by PNT presents strong evidence for its existence.

Table 2. The comparison between the values of three AHNs detected with PNT and the amplitudes of the 1-31 Hz EEG data for the sensor pair F4 and O2

	1-31 Hz EEG Amplitudes		3-*D* Values from PNT	
time (sec)	O2	F4	O2	F4
1.66	-8.029	5.654	0.976607143616050	0.976608882839799
12.65	-2.001	-4.622	0.984382629815184	0.984375119249569
14.48	-0.3727	0.2089	0.999775830582554	0.999781126238373

As another control measure, the raw EEG values from all the channels are cross-correlated at each time-step to identify the potential similarities. As an example, raw EEG values are displayed for the concurrent AHN pair (Fig. 10). No correlation was detected between the raw EEG channels, which verifies that the PNT is capable of detecting the connections established between the remote neural communities, using complex analysis. These deductions were satisfactory to conclude that connections are established between the remote communities, which AHNs not only exist but also have significant importance.

There are a few other deductions worth mentioning. The processed data which was filtered between 1-31 Hz, is the most suitable band for the PNT algorithm, showed the difference in engagement of the neural communities in resting and active brain stages. The difference in AHN counts are not consistent with that of the 1-31 Hz band when the 1-60 Hz band is examined (i.e. gamma wave band is included). Therefore, our results support the idea that not all neuroscientists are convinced of the existence of gamma waves, which are thought to be the artifact of the electromyographic activity [27, 28, 29].

It was observed and previously mentioned that processing a shorter EEG signal might bias the results. Since EEG data is non-stationary [26], selection of the Hilbert window plays a crucial role in calculating the AHN counts. Selecting a shorter Hilbert window results in drastically fewer AHNs because it fails to accurately detect the changes in the frequency content of the EEG data for a specific stimulus. Since the method intended to compare the AHN counts during the resting and active stages, the resting period is characterized as one stimulus while the active period is characterized as another. Therefore, the Hilbert window size was selected according to the length of these stimuli for the experimentation. For example, doubling the size of the Hilbert window increased the AHN counts by three to four times in both stages. Therefore, the mathematical model provided in this study to validate the existence of the antipodal connectivity structure is satisfactory because not only does raw EEG data show no correlation but also antipodal connectivity structure conforms to the nonlinearity principle [26] of the brain's cognitive processing.

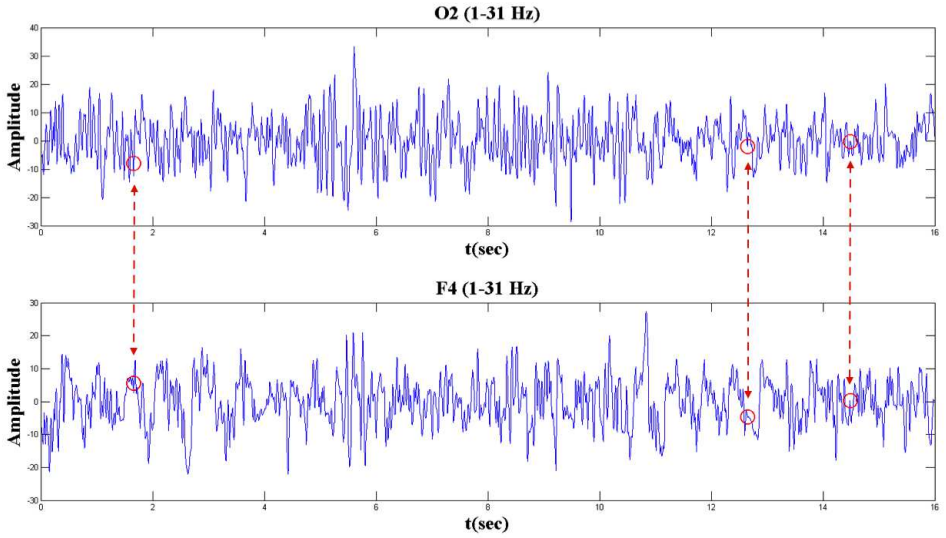

Figure 10. The amplitudes of the 1-31 Hz EEG values are marked with red circles for the concurrent AHN pair detected by the Sensors F4 and O2 at t=1.66, 12.65, 14.48 seconds

Neural activities are evolving in an organized fashion. In recent studies [6, 8], confirmed this evolution in focusing on the cortical functional connectivity, known as default network [30, 31, 32, 33, 34, 35, 36] and the interactions in the spatial-temporal domain. While investigating the regional connectedness by modeling the interactions, we realized a unique set of dynamic coupling reflecting the existence of antipodal structures among regions.

6. Conclusions

Borsuk-Ulams antipodal symmetry theory was adapted to establish the mathematical foundation for the PNT model. The PNT was tested on the EEG data collected in 50 experiments. A test procedure was established to distinguish the AHN counts during resting and active stages of the brain. According to these results, AHNs increase when brain is engaged with tasks such as problem solving and/or focused attention. There are no certain number of AHNs for each task due to two immediate factors;

1. the limited number of EEG data sets,
2. unique processing characteristics of each brain.

There are possibly additional factors that play a key role in AHN counts. However; this will require more testing and more detailed investigation. The precision of the system is also a key factor in determining the occurrence rate of antipodal connectivity, which was kept at hundred thousandths (10^{-5}).

The occurrence rate of antipodal connectivity is not random but depends on the stimuli and the selection of Hilbert transform window size. This is due to the non-stationary behavior of the electrical activity, which also causes antipodal connectivity to be a nonlinear process. Nonlinearity and lack of randomness of antipodal connectivity is substantially correlated with the previously proven theories.

Our results indicated that the AHN counts are more reliable between the 1-31 Hz band. This frequency band corresponds to the frequency band of the EEG signals, delta through beta, associated with the different stages, such as mediation through problem solving, respectively, but the upper limit of this band is usually at 38-40 Hz (beta waves). This suggests that the activity bandwidth may actually be shorter.

Acknowledgments

The authors thank Dr. Eric Kaufmann in the Department of Mathematics and Statistics at UALR for his assistance in mathematical concepts. For this study, Human Subject Use authorization was obtained for the data recording.

References

1. Chen ZJ, He Y, Rosa-Neto P, et al. (2008) Revealing modular architecture of human brain structural networks by using cortical thickness from MRI. *Cerebral cortex* 18: 2374-2381.
2. Ferri R, Rundo F, Bruni O, et al. (2008) The functional connectivity of different EEG bands moves towards small-world network organization during sleep. *Clinical Neurophysiology* 119: 2026-2036.
3. Meunier D, Achard S, Morcom A, et al. (2009) Age-related changes in modular organization of human brain functional networks. *Neuroimage* 44: 715-723.
4. Niedermeyer E, da Silva FL (2005) Electroencephalography: basic principles, clinical applications, and related fields: Lippincott Williams & Wilkins.
5. Nigam S, Shimono M, Ito S, et al. (2016) Rich-Club Organization in Effective Connectivity among Cortical Neurons. *The Journal of Neuroscience* 36: 670-684.
6. Hagmann P, Cammoun L, Gigandet X, et al. (2008) Mapping the structural core of human cerebral cortex. *PLoS Biol* 6: e159.
7. Rubinov M, Sporns O (2010) Complex network measures of brain connectivity: uses and interpretations. *Neuroimage* 52: 1059-1069.
8. Sporns O, Tononi G, Kotter R (2005) The human connectome: a structural description of the human. *Brain PLos Comput Biol(2005)* 1.
9. Leergaard TB (2012) Mapping the connectome: multi-level analysis of brain connectivity: Frontiers E-books.
10. Balanis CA (2012) Advanced engineering electromagnetics: Wiley Online Library.
11. Feynman RP, Leighton RB, Sands M (2013) The Feynman Lectures on Physics, Desktop Edition Volume I: Basic Books.
12. Serway R, Jewett J (2013) Physics for scientists and engineers with modern physics: Cengage learning.
13. Baumann SB, Wozny DR, Kelly SK, et al. (1997) The electrical conductivity of human cerebrospinal fluid at body temperature. *Biomedical Engineering, IEEE Transactions* on 44: 220-223.

14. Prescott T (2002) Extensions of the Borsuk-Ulam Theorem. Harvey Mudd College, http://citeseerx.ist.psu.edu.

15. Browder A (2006) Complex Numbers and the Ham Sandwich Theorem. *The American Mathematical Monthly*: 935-937.

16. Matousek J (2008) Using the Borsuk-Ulam theorem: lectures on topological methods in combinatorics and geometry: Springer Science & Business Media.

17. Aler R, Galvn IM, Valls JM (2012) Applying evolution strategies to preprocessing EEG signals for braincomputer interfaces. *Information Sciences* 215: 53-66.

18. Yang S, Deravi F. Wavelet-based EEG preprocessing for biometric applications; 2013. IEEE. pp. 43-46.

19. Hahn SL (1996) Hilbert transforms in signal processing: Artech House on Demand.

20. Yuvaraj R, Murugappan M, Ibrahim NM, et al. (2014) On the analysis of EEG power, frequency and asymmetry in Parkinsons disease during emotion processing. *Behav brain Funct* 10: 12.

21. Sanei S (2013) Adaptive processing of brain signals: John Wiley & Sons.

22. Iversen JR, Makeig S (2014) MEG/EEG Data Analysis Using EEGLAB. *Magnetoencephalography*: Springer. pp. 199-212.

23. Nater UM, Abbruzzese E, Krebs M, et al. (2006) Sex differences in emotional and psychophysiological responses to musical stimuli. *International journal of psychophysiology* 62: 300-308.

24. KABUTO M, KAGEYAMA T, NITTA H (1993) EEG Power Spectrum Changes due to Listening to Pleasant Musics and Their Relation to Relaxation Effects. *Nippon Eiseigaku Zasshi* 48: 807-818.

25. Delorme A, Makeig S (2004) EEGLAB: an open source toolbox for analysis of single-trial EEG dynamics including independent component analysis. *Journal of neuroscience methods* 134: 9-21.

26. Sanei S, Chambers JA (2013) EEG signal processing: John Wiley & Sons.

27. Whitham EM, Lewis T, Pope KJ, et al. (2008) Thinking activates EMG in scalp electrical recordings. *Clinical Neurophysiology* 119: 1166-1175.

28. Whitham EM, Pope KJ, Fitzgibbon SP, et al. (2007) Scalp electrical recording during paralysis: quantitative evidence that EEG frequencies above 20Hz are contaminated by EMG. *Clinical Neurophysiology* 118: 1877-1888.

29. Yuval-Greenberg S, Tomer O, Keren AS, et al. (2008) Transient induced gamma-band response in EEG as a manifestation of miniature saccades. *Neuron* 58: 429-441.

30. Fox MD, Raichle ME (2007) Spontaneous fluctuations in brain activity observed with functional magnetic resonance imaging. *Nature Reviews Neuroscience* 8: 700-711.

31. Shulman GL, Fiez JA, Corbetta M, et al. (1997) Common blood flow changes across visual tasks: II. Decreases in cerebral cortex. *Journal of cognitive neuroscience* 9: 648-663.

32. Raichle ME, MacLeod AM, Snyder AZ, et al. (2001) A default mode of brain function. *Proceedings of the National Academy of Sciences* 98: 676-682.

33. Greicius MD, Krasnow B, Reiss AL, et al. (2003) Functional connectivity in the resting brain: a network analysis of the default mode hypothesis. *Proceedings of the National Academy of Sciences* 100: 253-258.

34. Fox MD, Snyder AZ, Zacks JM, et al. (2006) Coherent spontaneous activity accounts for trial-to-trial variability in human evoked brain responses. *Nature neuroscience* 9: 23-25.

35. Fox MD, Snyder AZ, Vincent JL, et al. (2005) The human brain is intrinsically organized into dynamic, anticorrelated functional networks. *Proceedings of the National Academy of Sciences of the United States of America* 102: 9673-9678.

36. Fox MD, Corbetta M, Snyder AZ, et al. (2006) Spontaneous neuronal activity distinguishes human dorsal and ventral attention systems. *Proceedings of the National Academy of Sciences* 103: 10046-10051.

AIMS Press